Published in final edited form as:
Arch Ophthalmol. 2012 April ; 130(4): 440–445. doi:10.1001/archophthalmol.2011.378.

Characterization of Limbal Stem Cell Deficiency by In Vivo Laser Scanning Confocal Microscopy:

A Microstructural Approach

Sophie X. Deng, MD, PhD, **Kunjal D. Sejpal, DNB, FRCS**, **Qiongyan Tang, MD**, **Anthony J. Aldave, MD**, **Olivia L. Lee, MD**, and **Fei Yu, PhD**
The Jules Stein Eye Institute, David Geffen School of Medicine (Drs Deng, Sejpal, Tang, Aldave, and Lee), and Department of Biostatistics (Dr Yu), University of California, Los Angeles

Abstract

Objective—To evaluate the cellular changes in the corneal epithelium and surrounding structures in limbal stem cell deficiency (LSCD) by using in vivo laser scanning confocal microscopy.

Methods—This was a prospective comparative study that included 27 eyes of 20 patients with LSCD and 12 eyes of 10 healthy subjects. All subjects underwent slitlamp examination, and LSCD was classified into 3 groups on the basis of clinical presentation. Confocal imaging of the central cornea and 4 locations of limbus was performed. Morphologic characteristics of the corneal epithelium were studied. The basal epithelial cell density and subbasal nerve density in the central cornea were calculated, and a potential correlation between the decrease in basal epithelial cell density and subbasal nerve density in LSCD was investigated.

Results—The wing and basal epithelial cells became progressively metaplastic, and the basal epithelial cell density and subbasal nerve density in the early and intermittent stages decreased significantly compared with controls (all $P<.01$). Normal basal epithelial cell morphology was completely lost and subbasal nerves were absent in the late stage of LSCD. The decrease in basal cell density correlated with the decrease in subbasal nerve density in patients with LSCD ($P=.03$).

Conclusions—There are significant microstructural changes associated with early LSCD. These cellular changes could help to understand the disease process and classify and monitor limbal stem cell dysfunction.

A transparent corneal epithelial surface is maintained by the corneal epithelial stem cells, and it is believed that they are located at the basal layer of the limbal epithelium.[1–3] When the limbal stem cells are deficient, the conjunctival epithelial cells invade onto the corneal surface and lead to decreased vision. Limbal stem cell deficiency (LSCD) is seen in many ocular disorders such as chemical injury, multiple intraocular surgeries, and Stevens-Johnson syndrome.[4] The diagnosis and management of LSCD remain very challenging. The diagnosis of LSCD is mainly based on history and clinical presentation. The classic clinical signs of LSCD include stippling and late fluorescein staining, epithelial opacity/late fluorescein staining in a vortex pattern, recurrent epithelial breakdown, and fibrovascular pannus on the corneal surface.[5,6] At the time of presentation, patients with partial or sectoral LSCD often have very subtle changes that may be missed by clinical examination alone.

Correspondence: Sophie X. Deng, MD, PhD, Jules Stein Eye Institute, 100 Stein Plaza, Los Angeles, CA 90095, (deng@jsei.ucla.edu).

Financial Disclosure: None reported.

Online-Only Material: The eFigure and eTable are available at http://www.archophthalmol.com.

Impression cytology is an accepted diagnostic test for LSCD,[4] but the false-negative rate is high partly because of the coexisting goblet cell deficiency in many disorders. Keratin 19 has been proposed as a marker for conjunctival epithelial cells in the diagnosis of LSCD.[7,8] However, its expression specificity is controversial.[9–11] Therefore, a sensitive test to quantify limbal stem cell damage is not possible clinically because of the lack of a classification system.

In vivo laser scanning confocal microscopy, which provides high-resolution images of the ocular surface at the cellular level, is a very powerful tool to evaluate microstructure. This technique has gained wide popularity among clinicians as a method to evaluate various physiologic and pathologic changes in the cornea, conjunctiva, and limbus.[12–16] A study by Vera et al[15] of the corneal changes in chronic Stevens-Johnson syndrome and toxic epidermal necrolysis showed abnormalities in the corneal epithelium and an absence of the subbasal nerve plexus in those patients with advanced LSCD. To our knowledge, cellular changes in various stages of LSCD have not been described and quantified. The purpose of the study described herein was to elucidate and quantify the microstructural changes in the corneal epithelium and subbasal nerve plexus in the early stages of LSCD.

METHODS

PATIENT IDENTIFICATION AND CLINICAL CLASSIFICATION OF LSCD

This study was performed with approval of the institutional review board at the University of California, Los Angeles. Proper consent was obtained. Subjects were examined by slitlamp biomicroscopy, and slitlamp photographs were taken. The diagnosis of LSCD was based on clinical evaluation, and the severity of the disease was categorized into 3 stages on the basis of clinical presentation: (1) the early stage, characterized by the stippling or late fluorescein staining and a dull reflex; (2) the intermediate stage, characterized by persistent late fluorescein staining in a vortex pattern associated with depression of the epithelial surface; and (3) the late stage, characterized by vortex epithelial opacity as seen in the intermediate group with a history of recurrent epithelial defect with or without conjunctivalization/vascularization of the cornea. Those subjects who had undergone penetrating keratoplasty were excluded from the quantitative analysis of basal cell density (BCD) and subbasal nerve density (SND). The control group consisted of subjects who did not have a history of eye disease and were free of any ocular symptoms or abnormality of the corneal epithelium as seen during slitlamp examination. Normal subjects who had undergone any ocular surface surgery were excluded.

CONFOCAL IMAGING

In vivo laser scanning confocal microscopy was performed with the Heidelberg Retina Tomograph III Rostock Cornea Module (Heidelberg Engineering GmBH). All eyes were anesthetized with proparacaine, 0.5% (Alcon Laboratories). Hydroxypropyl methylcellulose (Novartis Ophthalmics, Inc) was applied. Images of the central cornea and 4 areas of the limbus (superior, temporal, inferior, and nasal) were obtained. The location of imaging was confirmed visually by the red aiming beam and through the side camera of the Heidelberg Retina Tomograph III.

IMAGE ANALYSIS

The morphology of the cells in the wing and basal epithelial layers and of the nerves in the subbasal nerve plexus was examined. The epithelial cell layer just above the subbasal nerve plexus was defined as the basal layer. Three images that showed a clear morphology of the basal epithelial layer were selected for BCD analysis. Two independent observers (K.D.S. and O.L.L.) manually counted cells according to the manufacturer’s instructions for a cell

count in a masked fashion. Similarly, 3 images that demonstrated the highest number of subbasal nerve plexuses were selected to obtain the total SND. The SND was obtained by dividing the nerve counts by the imaged area (0.16 mm^2).

STATISTICAL ANALYSES

Statistical analyses were performed with SAS version 9.1 (SAS Institute, Inc). The reliability of BCD and SND obtained by independent observers was assessed by using intraclass correlation coefficients from repeated-measures mixed-effect regression models. The average of the measurements from all 3 images for each eye was compared by using Kruskal-Wallis tests. Any *P* value less than .05 was considered statistically significant. The Spearman correlation coefficient was calculated between the BCD and SND in the control and LSCD groups.

RESULTS

PATIENT CHARACTERISTICS

A total of 39 eyes were evaluated in this study: 27 eyes of 20 patients with LSCD and 12 eyes of 10 control subjects. Patient demographic features, diagnoses, and clinical presentations are summarized in the Table. The mean age of subjects was 59.1 years (range, 22–94 years) in the LSCD group and 48.8 years (range, 27–88 years) in the control group. There was no statistically significant difference in age and sex between the control and LSCD groups (*t* test, *P*=.25). Representative slitlamp photos of the corneas at each of the 3 stages of LSCD are shown in Figure 1. Limbal stem cell deficiency was classified as early stage in 10 eyes, intermediate stage in 13 eyes, and late stage in 4 eyes. The most common etiologies of LSCD were Stevens-Johnson syndrome and multiple surgeries (6 of 27, 22%) followed by contact lens wear (5 of 27, 19%) (eTable, http://www.archophthalmol.com).

MORPHOLOGY OF NORMAL CORNEA EPITHELIUM

The corneal epithelium consists of 3 layers: the superficial, wing/intermediate, and basal layers. The superficial epithelial cells were large with distinct cell borders and dark nuclei with a perinuclear halo. The wing cells were smaller than the superficial cells and had hyporeflective cytoplasm and a well-demarcated hyperreflective cell border. Three to 5 layers of epithelial cells were within this middle portion of the epithelium. The cells became smaller as the depth of the wing layer increased (Figure 2A, top left panel). The basal cells were smaller than the wing cells and highly compact with uniform polygonal shape. The cell nuclei were not normally visible (Figure 2A, top middle panel). The subbasal nerves were long and relatively straight (Figure 2A, top right panel).

MORPHOLOGIC CHANGES IN THE CORNEAS OF PATIENTS WITH LSCD

The wing layer was affected in half of the patients. The nuclei became hyperreflective and visible at the more superficial layer in early LSCD (Figure 2A, second row). The cell size and shape were fairly normal. The basal cells became slightly bigger, and some exhibited prominent nuclei. The cell border was less distinct than that seen in healthy subjects. In the intermediate group, these morphologic changes became more advanced (Figure 2A, third row). The epithelial cells at all levels were affected. The nuclei were very prominent and the cell size increased. The cell border became less distinct at the basal layer. Epithelial cells in the late stage showed significant metaplasia. The normal morphology of basal and wing epithelial cells was lost. Only a couple layers of metaplastic cells were detected (Figure 2A, bottom row). Subbasal fibrosis and neovascularization were observed in this stage. The SND decreased in patients with LSCD. No subbasal nerves were detected in patients with late-stage LSCD.

The morphologic changes in the limbal epithelium were similar to those observed in the cornea (Figure 2B). The palisades of Vogt were absent at the affected sector of the limbus, and there was an increase in reflectivity at the immediate subbasal layer. The vascular fibrotic tissues completely replaced the normal limbal epithelium at the late stage of LSCD.

QUANTITATION OF CELLULAR CHANGES IN THE CORNEA

To quantify the microstructural changes in the corneas with LSCD, we assessed the BCD and SND in the normal and LSCD groups. The border of the basal cells at the late stage was indistinct and thus prevented an accurate cell count. In addition, there was a complete absence of nerve fibers in these patients.

Using interclass correlation coefficients, we found good agreement in the BCDs (eFigure, A) and SNDs (eFigure, B) between these 2 observers. The mean (SD) BCD was 9373 (483) cells/mm^2 in healthy subjects and 5029 (2323) cells/mm^2 in the LSCD group. Analysis of BCD within the subgroups of LSCD showed that the mean (SD) BCD was 5850 (2226) cells/mm^2 in early-stage LSCD and 4583 (2210) cells/mm^2 in intermediate-stage LSCD. The mean (SD) SND was 101.3 (37.7) nerves/mm^2 in healthy subjects, 31.9 (35.8) nerves/mm^2 in the LSCD group, 42.7 (50.1) nerves/mm^2 in early-stage LSCD, and 23.7 (15.1) nerves/mm^2 in intermediate-stage LSCD. The BCD (Figure 3A) and SND (Figure 3B) were significantly less in patients with LSCD than in the healthy subjects (Wilcoxon rank sum test, $P<.01$ for all comparisons). There were further decreases in the BCD and SND in the intermediate stage, although the differences between the early and intermediate groups did not reach statistical significance ($P=.37$ and $P=.88$, respectively).

There was no evidence of statistically significant correlations between BCD and SND in healthy control subjects (Spearman correlation coefficient −0.063; $P=.85$), but there was a significant correlation between the decrease in BCD and the decrease in SND (0.47; $P=.03$) in patients with LSCD by Spearman correlation coefficient.

Receiver operating characteristic curve analysis of the BCD and SND in the control subjects and those with LSCD revealed the cutoff value for the BCD (Figure 4A) was 7930 cells/mm^2, and the resulting sensitivity and specificity were 95.5% and 100%, respectively. The lower cutoff value for the SND (Figure 4B) was 53 nerves/mm^2, and resulting sensitivity and specificity were 87.0% and 91.7%, respectively. On the basis of these results, a decrease in the BCD of more than 15.4% and a decrease in the SND of more than 47.7% might be associated with the earliest signs of limbal stem cell dysfunction.

COMMENT

Using laser scanning confocal microscopy, we analyzed in detail the cellular structure of the corneal epithelial layers and subbasal nerve plexus in healthy subjects and patients with various degrees of LSCD. Increases in basal epithelial cell size, decreases in innervation, and metaplastic changes in the basal epithelial cells including prominent nuclei and loss of distinct cell borders were associated with early LSCD. To our knowledge, this study is the first to characterize the microstructural changes in patients with various degree of LSCD.

Compared with the healthy control subjects, those with early-stage LSCD had an average of 38% reduction in BCD and a 58% reduction in SND. A decrease in BCD is expected as a result of the failure of stem cell function; however, loss of innervation is a surprising finding in LSCD. It is also very intriguing that the decrease in the BCD is significantly correlated with the decrease in the SND in LSCD. Corneal nerve fibers support the maintenance of healthy corneal epithelial cells by secreting trophic factors such as neuropeptides and neurotransmitters that stimulate epithelial cell growth, proliferation, regeneration,

differentiation, and possibly migration.[17–19] Corneal and limbal epithelial cells also secrete glial cell–derived nerve growth factors and nerve growth factors that also have trophic effects on nerve fibers.[20] It is unclear whether degeneration of the subbasal nerve fibers leads to a depletion of basal epithelial cells or the loss of normal corneal epithelial cells leads to degeneration of the subbasal nerve fibers.

Slight decreases in both BCD and SND have been observed in patients with keratoconus,[21] active atopic conjunctivitis,[22] and diabetes.[23] The average reduction in BCD and SND is far greater in LSCD than in these conditions. In addition, the changes in epithelial cell morphology are not reported in keratoconus and diabetes. Atopic conjunctivitis is one of the known etiologies of LSCD. The chronic severe inflammation on the ocular surface causes damages to the corneal epithelium, limbal stem cells, and the stem cell niche. It is not surprising that in active severe atopic conjunctivitis both cell densities are affected.

Many of our patients also had concurrent dry eye syndrome, a condition that has been extensively evaluated by laser scanning confocal microscopy. The BCD either remains unchanged[24] or increases slightly[25] in patients with dry eye syndrome alone. There are conflicting results regarding the SND in dry eye syndrome; Zhang et al[26] noted a significant increase, whereas others showed a decrease or no change in the nerve density.[25,27] The superficial epithelial layer is affected in dry eye syndrome, and therefore, we specifically only focused on the changes in the wing and basal layers in the current study to avoid including changes that were not associated with LSCD. Patients with dry eye syndrome in the absence of LSCD do not have significant metaplasia. Although LSCD is attributed to several different etiologies in the current study (eg, contact lens wear, multiple surgeries, and drug toxic effects), none of them in the absence of LSCD was associated with decreases in both BCD and SND and changes in the epithelial morphology. Despite the different diagnoses among our patients, a decrease in both the BCD and SND and changes in the morphology of corneal and limbal epithelial cells are the common phenomena in all of these patients who share a common condition, LSCD. This similarity further supports our conclusion that our findings are the results of LSCD and not due to different conditions.

Currently, the diagnosis of LSCD relies on clinical findings and is confirmed by impression cytology that demonstrates the presence of goblet cells on the cornea.[4] It is possible that the migration of goblet cells onto the cornea is a rather late phenomenon preceded by corneal epithelial cell metaplasia, a hypothesis that is supported by the results of our current study. When LSCD was in the early stage, the morphology of the basal epithelial cells began to change. However, the phenotype of the cells remained corneal not conjunctival, as indicated by the classic polygonal shape. The cells became conjunctival-like only in the later stages of LSCD.

The current study found that a similar change in the morphology occurs in the limbal epithelial cells. These alterations became more prominent with the advancement of the disease, and changes in the underlying stroma also occurred, including the loss of the palisades of Vogt, an anatomic landmark of the posterior limbus. The observation that the BCD is higher in the anterior limbus than the posterior location[12] further complicates the quantitation of the cell count in LSCD when the palisades of Vogt is absent. Our current study focused on the findings in the central cornea because the BCD and SND can be easily quantified with the same standard, and they likely represent the overall limbal stem cell function. However, there is limitation of the current study because of the lack of an established standard that can be used to confirm the degree of limbal stem cell deficiency. A more comprehensive staging of LSCD will require correlation of the limbal microstructural changes with the clinical presentation and confirmation with histopathologic study. In addition, the current study is an initial investigation and a larger prospective study would be

necessary to further delineate the gradual decrease of BCD and SND in the early and intermediate stage of LSCD.

In conclusion, to our knowledge, we report the first in vivo laser scanning confocal microscopy study to elucidate and characterize the microstructural changes in LSCD. A better knowledge of these cellular changes could help us to understand the underlying disease process. The finding reported herein could also serve as a useful foundation for the development of a noninvasive method to quantify and monitor the progression of LSCD and response to treatment.

Acknowledgments

Funding/Support: This study was funded by an Investigator Award from Prevent Blindness America (Dr Deng).

Additional Contributions: We thank Joel Sugar, MD, for critical reading of the manuscript.

REFERENCES

1. Schermer A, Galvin S, Sun TT. Differentiation-related expression of a major 64K corneal keratin in vivo and in culture suggests limbal location of corneal epithelial stem cells. J Cell Biol. 1986; 103(1):49–62. [PubMed: 2424919]
2. Lavker RM, Tseng SC, Sun TT. Corneal epithelial stem cells at the limbus: looking at some old problems from a new angle. Exp Eye Res. 2004; 78(3):433–446. [PubMed: 15106923]
3. Tseng SC. Concept and application of limbal stem cells. Eye (Lond). 1989; 3(pt 2):141–157. [PubMed: 2695347]
4. Puangsricharern V, Tseng SC. Cytologic evidence of corneal diseases with limbal stem cell deficiency. Ophthalmology. 1995; 102(10):1476–1485. [PubMed: 9097795]
5. Dua HS, Azuara-Blanco A. Limbal stem cells of the corneal epithelium. Surv Ophthalmol. 2000; 44(5):415–425. [PubMed: 10734241]
6. Dua HS, Gomes JA, Singh A. Corneal epithelial wound healing. Br J Ophthalmol. 1994; 78(5):401–408. [PubMed: 8025077]
7. Sacchetti M, Lambiase A, Cortes M, et al. Clinical and cytological findings in limbal stem cell deficiency. Graefes Arch Clin Exp Ophthalmol. 2005; 243(9):870–876. [PubMed: 15778841]
8. Donisi PM, Rama P, Fasolo A, Ponzin D. Analysis of limbal stem cell deficiency by corneal impression cytology. Cornea. 2003; 22(6):533–538. [PubMed: 12883346]
9. Chen Z, de Paiva CS, Luo L, Kretzer FL, Pflugfelder SC, Li DQ. Characterization of putative stem cell phenotype in human limbal epithelia. Stem Cells. 2004; 22(3):355–366. [PubMed: 15153612]
10. Barbaro V, Ferrari S, Fasolo A, et al. Evaluation of ocular surface disorders: a new diagnostic tool based on impression cytology and confocal laser scanning microscopy. Br J Ophthalmol. 2010; 94(7):926–932. [PubMed: 19740872]
11. Ramirez-Miranda A, Nakatsu MN, Zarei-Ghanavati S, Nguyen CV, Deng SX. Keratin 13 is a more specific marker of conjunctival epithelium than keratin 19. Mol Vis. 2011; 17:1652–1661. [PubMed: 21738394]
12. Patel DV, Sherwin T, McGhee CN. Laser scanning in vivo confocal microscopy of the normal human corneoscleral limbus. Invest Ophthalmol Vis Sci. 2006; 47(7):2823–2827. [PubMed: 16799020]
13. Kaufman SC, Musch DC, Belin MW, et al. Confocal microscopy: a report by the American Academy of Ophthalmology. Ophthalmology. 2004; 111(2):396–406. [PubMed: 15019397]
14. Niederer RL, Perumal D, Sherwin T, McGhee CN. Age-related differences in the normal human cornea: a laser scanning in vivo confocal microscopy study. Br J Ophthalmol. 2007; 91(9):1165–1169. [PubMed: 17389741]
15. Vera LS, Gueudry J, Delcampe A, Roujeau JC, Brasseur G, Muraine M. In vivo confocal microscopic evaluation of corneal changes in chronic Stevens-Johnson syndrome and toxic epidermal necrolysis. Cornea. 2009; 28(4):401–407. [PubMed: 19411958]

16. Eckard A, Stave J, Guthoff RF. In vivo investigations of the corneal epithelium with the confocal Rostock Laser Scanning Microscope (RLSM). Cornea. 2006; 25(2):127–131. [PubMed: 16371768]
17. Qi H, Li DQ, Bian F, Chuang EY, Jones DB, Pflugfelder SC. Expression of glial cell-derived neurotrophic factor and its receptor in the stem-cell-containing human limbal epithelium. Br J Ophthalmol. 2008; 92(9):1269–1274. [PubMed: 18723744]
18. Garcia-Hirschfeld J, Lopez-Briones LG, Belmonte C. Neurotrophic influences on corneal epithelial cells. Exp Eye Res. 1994; 59(5):597–605. [PubMed: 9492761]
19. You L, Kruse FE, Völcker HE. Neurotrophic factors in the human cornea. Invest Ophthalmol Vis Sci. 2000; 41(3):692–702. [PubMed: 10711683]
20. Qi H, Chuang EY, Yoon KC, et al. Patterned expression of neurotrophic factors and receptors in human limbal and corneal regions. Mol Vis. 2007; 13:1934–1941. [PubMed: 17982417]
21. Mocan MC, Yilmaz PT, Irkec M, Orhan M. In vivo confocal microscopy for the evaluation of corneal microstructure in keratoconus. Curr Eye Res. 2008; 33(11):933–939. [PubMed: 19085375]
22. Hu Y, Matsumoto Y, Adan ES, et al. Corneal in vivo confocal scanning laser microscopy in patients with atopic keratoconjunctivitis. Ophthalmology. 2008; 115(11):2004–2012. [PubMed: 18584874]
23. Chang PY, Carrel H, Huang JS, et al. Decreased density of corneal basal epithelium and subbasal corneal nerve bundle changes in patients with diabetic retinopathy. Am J Ophthalmol. 2006; 142(3):488–490. [PubMed: 16935596]
24. Benítez del Castillo JM, Wasfy MA, Fernandez C, Garcia-Sanchez J. An in vivo confocal masked study on corneal epithelium and subbasal nerves in patients with dry eye. Invest Ophthalmol Vis Sci. 2004; 45(9):3030–3035. [PubMed: 15326117]
25. Villani E, Galimberti D, Viola F, Mapelli C, Ratiglia R. The cornea in Sjogren's syndrome: an in vivo confocal study. Invest Ophthalmol Vis Sci. 2007; 48(5):2017–2022. [PubMed: 17460255]
26. Zhang M, Chen J, Luo L, Xiao Q, Sun M, Liu Z. Altered corneal nerves in aqueous tear deficiency viewed by in vivo confocal microscopy. Cornea. 2005; 24(7):818–824. [PubMed: 16160498]
27. Hoşal BM, Ornek N, Zilelioğlu G, Elhan AH. Morphology of corneal nerves and corneal sensation in dry eye: a preliminary study. Eye (Lond). 2005; 19(12):1276–1279. [PubMed: 15550934]

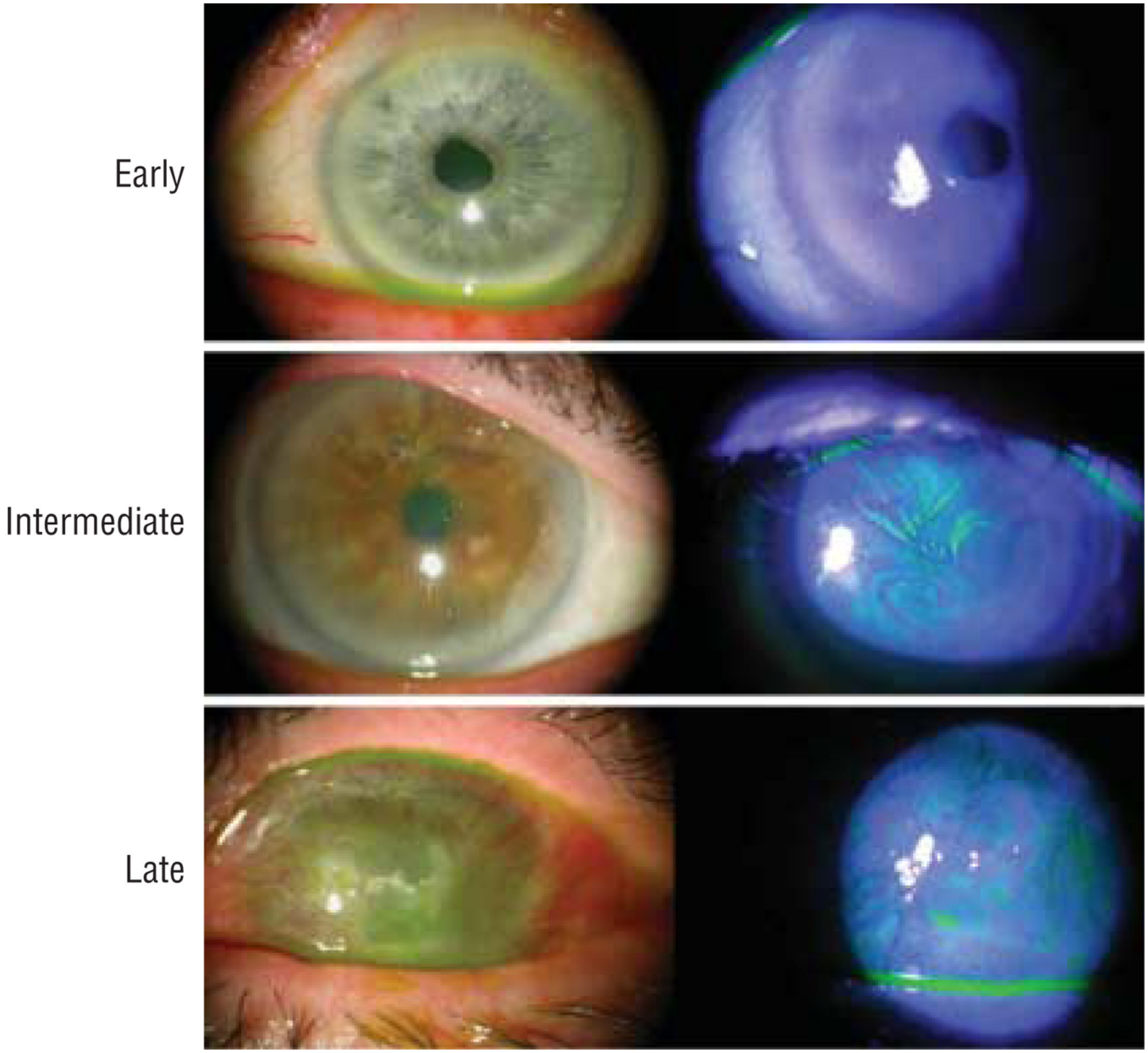

Figure 1.
Slitlamp photographs of eyes at early (top panel), intermediate (middle panel), and late (bottom panel) stages of limbal stem cell deficiency. The fluorescein staining patterns are shown in the right column.

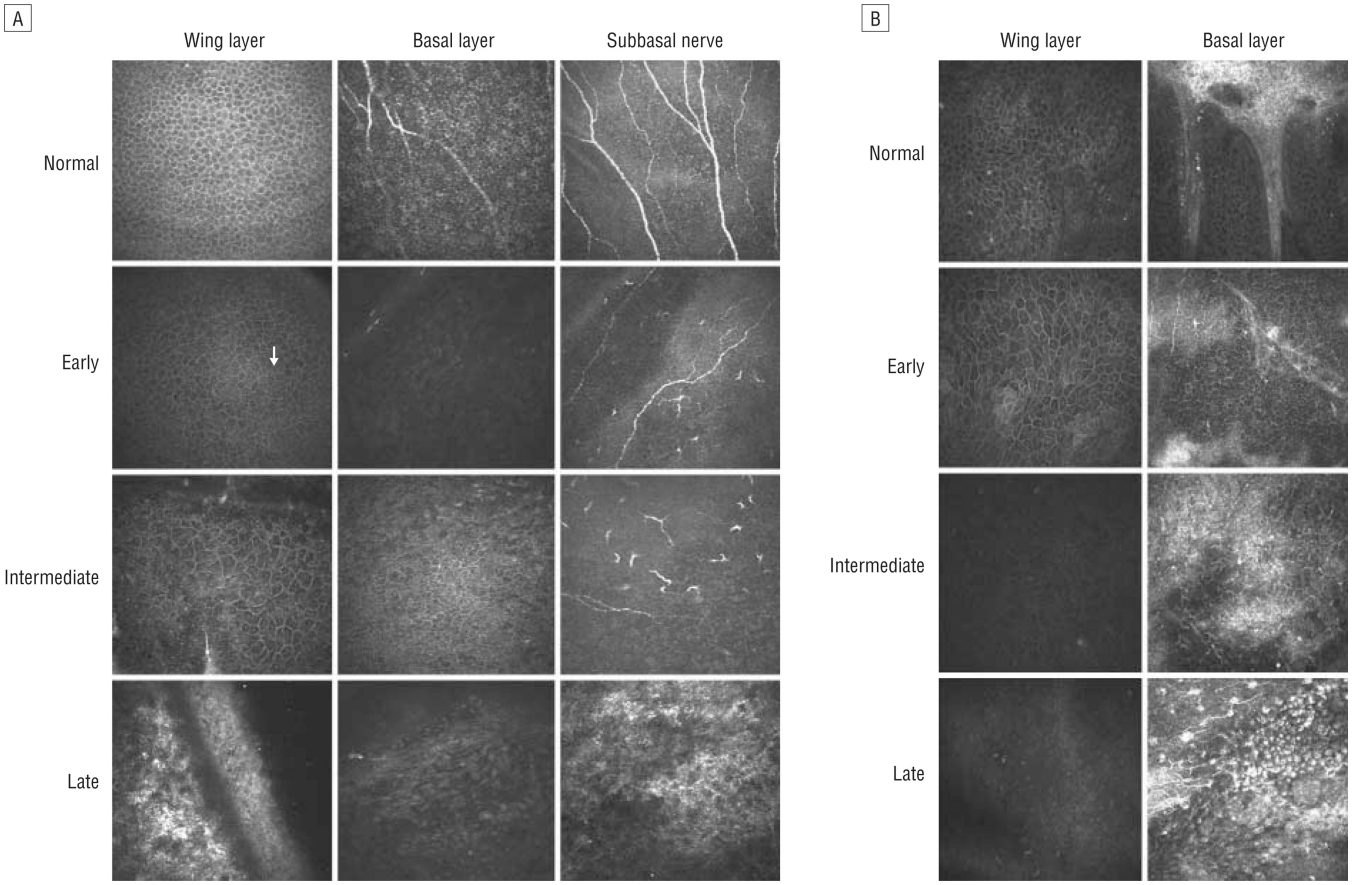

Figure 2.

Representative confocal images of the wing and basal epithelial layers and subbasal nerve plexus at different clinical stages of limbal stem cell deficiency. A, Images of the wing (left column) and basal epithelial (middle column) layers in the central cornea. The subbasal nerve plexus is also shown (right column). The arrow indicates prominent nuclei. B, Images of the wing (left column) and basal epithelial (right column) layers in the limbus.

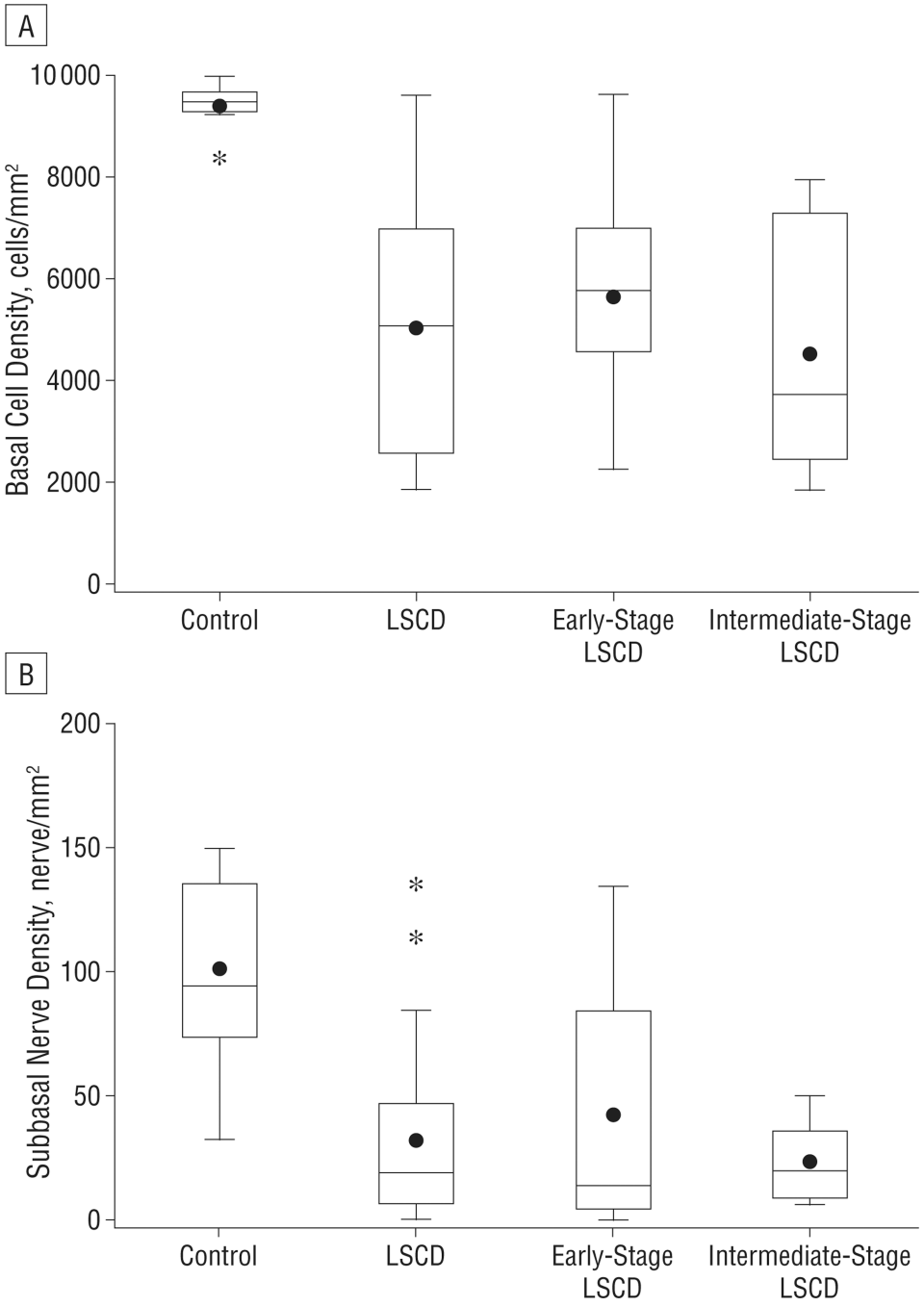

Figure 3.

Box and whisker plot of central corneal basal epithelial cell density (A) and subbasal nerve density (B). There was a significant decrease in basal cell density and subbasal nerve density in all patients with limbal stem cell deficiency (LSCD) and in the subgroups of early-stage and intermediate-stage LSCD compared with controls. *P<.001.

The dots indicate the mean.

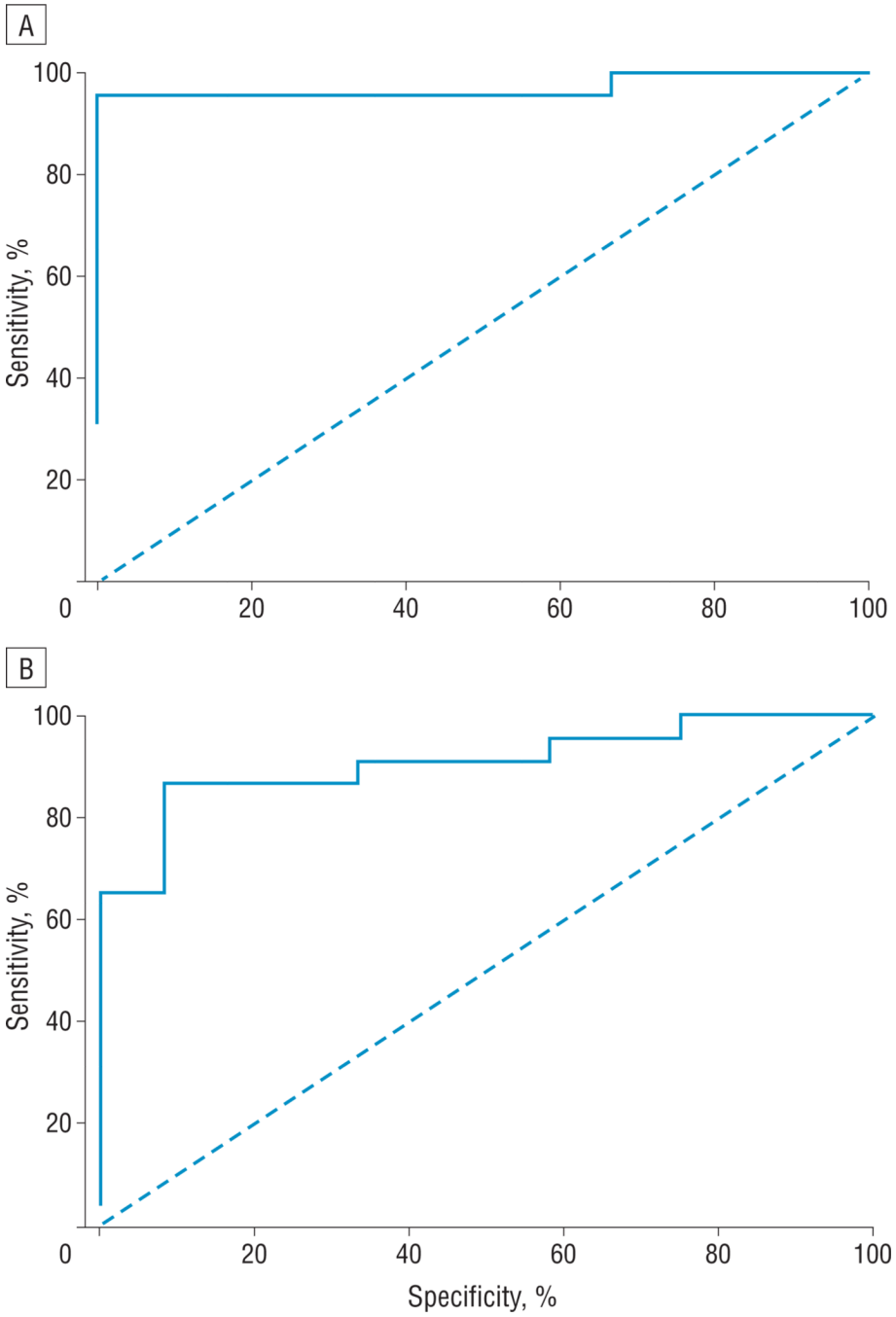

Figure 4.

Receiver operating characteristic curve for central corneal basal epithelial cell density (A) and subbasal nerve density (B). The lower cutoff basal epithelial cell density to diagnose limbal stem cell deficiency was 7930 cells/mm^2 and resulted in a 95.5% sensitivity and 100% specificity. The lower cutoff subbasal nerve density was 53 nerves/mm^2 and resulted in an 87.0% sensitivity and 91.7% specificity.

Table

Patient Demography and Clinical Presentation

Patient/Sex/Age, y	Diagnosis	Eye	Clinical Findings	Clinical Stage
1/M/48	SJS, DES	R	Mild superior stippling staining	Early
2/M/48	SJS, DES	L	Complete conjunctivalization	Late
3/M/44	SJS, DES	L	Mild stippling staining	Early
4/M/44	SJS, DES	R	Moderate superficial NV, moderate stippling staining	Intermediate
5/M/78	Multiple surgeries	L	Mild stippling staining	Early
6/M/78	Multiple surgeries	R	Superior vortex keratopathy	Intermediate
7/M/94	Drug toxic effects	R	Late fluorescein staining	Early
8/M/94	Drug toxic effects	L	Vortex keratopathy	Intermediate
9/M/50	Lichen planus, DES	R	Moderate peripheral NV	Early
10/F/59	Irradiation, chemotherapy, DES	R	Moderate diffuse staining	Early
11/F/59	Chemotherapy, DES	L	Moderate diffuse staining	Early
12/F/36	CL	L	Superior stippling staining	Early
13/F/36	CL	R	Superior vortex keratopathy	Intermediate
14/F/22	CL	R	Moderate diffuse staining	Early
15/F/22	CL	L	Moderate diffuse staining	Early
16/F/88	Neurotrophic keratopathy, DES	R	Epithelial irregularity, late staining	Intermediate
17/M/34	SJS, DES	R	Superior vortex keratopathy	Intermediate
18/M/44	SJS, DES	R	Moderate superficial pannus	Intermediate
19/F/59	Multiple surgeries	R	Inferior vortex keratopathy	Intermediate
20/M/92	Idiopathic	R	Vortex keratopathy	Intermediate
21/F/77	Multiple surgeries	R	Vortex keratopathy	Intermediate
22/M/60	Multiple surgeries	L	Vortex keratopathy	Intermediate
23/F/56	CL	R	Vortex keratopathy	Intermediate
24/F/83	Drug toxic effects, DES	L	Vortex keratopathy	Intermediate
25/F/71	Drug toxic effects, neurotrophic keratopathy	L	Peripheral NV, RED	Late
26/M/24	Chemical burn	R	Conjunctivilization	Late
27/M/25	Multiple surgeries	R	RED, conjunctivilization	Late

Abbreviations: CL, contact lens; DES, dry eye syndrome; NV, neovascularization; RED, recurrent epithelial defect; SJS, Stevens-Johnson syndrome.